COHERENT MARINE RADAR MEASUREMENTS OF PROPERTIES OF OCEAN WAVES AND CURRENTS

Dennis Trizna

Imaging Science Research, Inc.

1. INTRODUCTION

Marine radars offer the capability to image ocean wave propagation by virtue of repetitive coverage of the same scene. With a typical 1.25-s rotation period, ocean wave frequencies of 0.4 Hz can be measured unambiguously. Imaged areas of the order of ten square kilometers, allow the dynamics and kinematics of ocean wave fields to be measured with higher azimuthal resolution than traditional oceanographic instruments, such as buoys or pressure sensors.

Using the dispersion relation for shallow waves in coastal regions, ocean wave spectra and bathymetry can be estimated using non-coherent marine radars [1-5]. The derivation of wave height or wave height spectra from marine radar imagery has had some success by relating the radar echo intensity imagery of waves to wave height using an empirically derived modulation transfer function (MTF). More recently, using a radar scattering model's dependence of the radar scattering cross section on long wave slope [6], good results are reported in deep water for shipboard experiments, where winds and waves are typically in the same direction. However, in coastal waters, offshore winds blowing in a direction other than that of the incoming wave field can produces enhanced roughness on the front face of waves, resulting in a modulation of the radar wave field image that is not wave height dependent [7]. Fig. 1 shows such an example

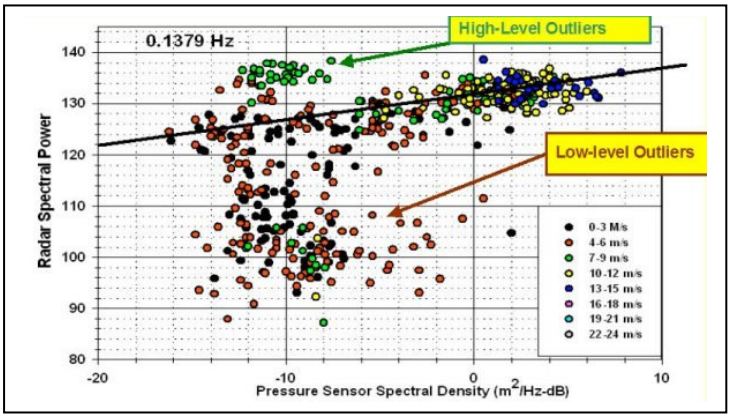

Figure 1. Radar vs. pressure sensor spectral peaks, sorted by winds speed, generally give good fits above 4 m/s. High-level outliers occur when winds blow opposite the wave direction, leading to overestimates of wave height from radar data. Low level outliers can occur due to coastal slicks.

A coherent radar can overcome these limitations using the direct measurement of the radial component of orbital wave velocity, accounting for Bragg scatter velocity. Radial orbital velocity will maximize and minimize at similar locations on long wave profiles as do radar echo intensity, so wave patterns should look very similar for the two. Thus, analysis methods similar to those used in non-coherent radar studies should be applicable to coherent radar data as well. We present recent experimental results on the retrieval of coastal ocean wave and current properties due to a storm over the Outer Banks of North Carolina in November of 2009.

2. COHERENT RADAR DESCRIPTION AND IMAGERY

A fully coherent marine radar was developed for imaging ocean wave orbital wave velocity with a 0.8-Hz radar rotation rate and 1.25-s image repetition period, providing a direct measurement of wave height profiles, without relying on the MTF as discussed above. A Koden marine radar was gutted of its components and replaced with microwave components to produce a fully coherent radar. The non-coherent 25-kilowatt magnetron was replaced with a 5-watt solid-state power amplifier. FM chirp pulse compression is used to improve the effective coherent output power, the waveform generated by the ISR Quadrapus transceiver PC card. Additional signal gain is achieved by summing successive echo waveforms in a FPGA on the transceiver card before recording the waveform to storage media. Typical operation uses a 50,000 Hz pulse repetition frequency (PRF) on transmit, sums 50 or 25 pulses, giving a 1 or 2 KHz record PRF, providing 22 to 25-dB gain, almost making up for the factor of 5,000 in transmitted peak power.

The recorded signal is the output intermediate frequency of the radar, with a single channel only, providing real data, typically at 1.5-m sample spacing at a 100-MHz sample rate. Pulse compression gives complex in-phase (I) and quadrature (Q) outputs at a 3-m spacing. The arctangent of the I/Q ratio for each range bin gives the phase of each. Phase difference, $d\phi$, between adjacent pulses provides a measure of rate of change of phase (rad/sec), or Doppler shift (Hz), $d\phi/dt = f_D$, by dividing this phase difference by the period between pulses. This in turn is related to the radial velocity of an echo by the Doppler equation:

$$V_D = f_D * \lambda/2$$

The radar was mounted on a tower at the end of the FRF pier, 600 m offshore. Cartesian images of intensity (left) and mean 2-pulse phase differences (right) are seen in Fig. 2, for one day during the passage of Hurricane Ida offshore in late November of 2009. The radial Doppler radial velocity scales from -8 ms/s to 8 m/s for the 1-KHz recording PRF. Note a slight mean offset in the phase image, which is due to a current from the north (top) running on that day.

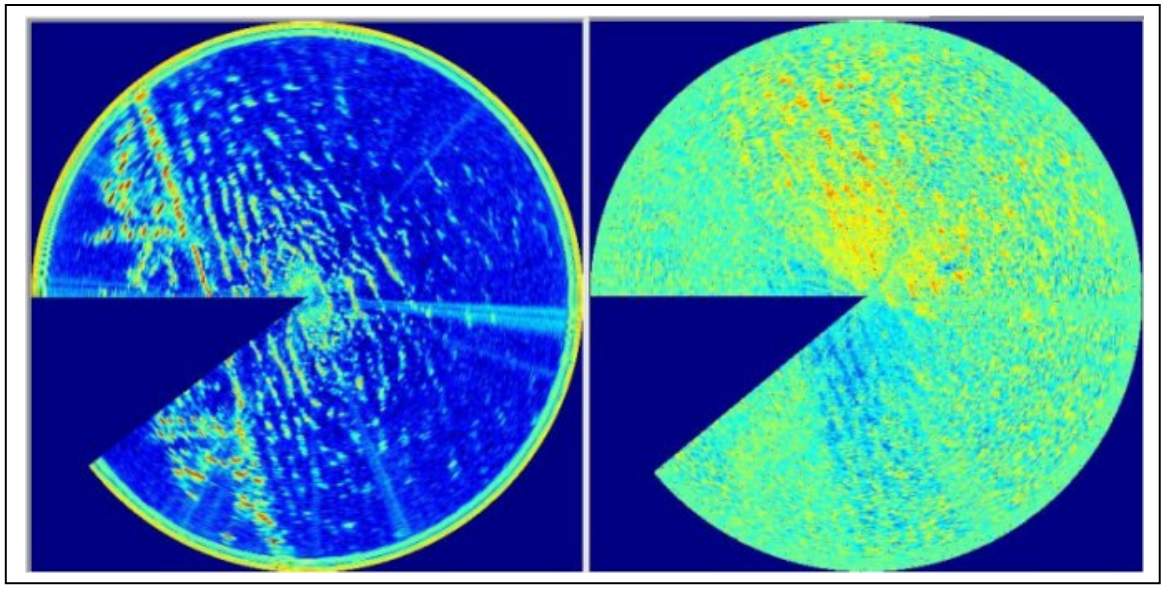

Fig. 2. Video image (left) and phase-difference image (right), 985 pixels or 2955-m diameter for each. 16x16-pixel windows were placed over the FRF pressure array for 3-D FFT analysis.

3. ANALYSIS RESULTS

3D-FFT analysis of 4 sets of 64 rotations produced radial velocity wave number spectra for each of 32 positive and negative frequencies ranging between -0.4 to 0.4 Hz, with symmetry across 0 frequency, resulting in just 32 frames of useful spectra. Fig. 3 shows and example of 8 of these 32 frequencies, user selectable, for phase-difference image processing. The coastline at the FRF is shore-normal at 68 deg, so true North is up in the spectra and images.

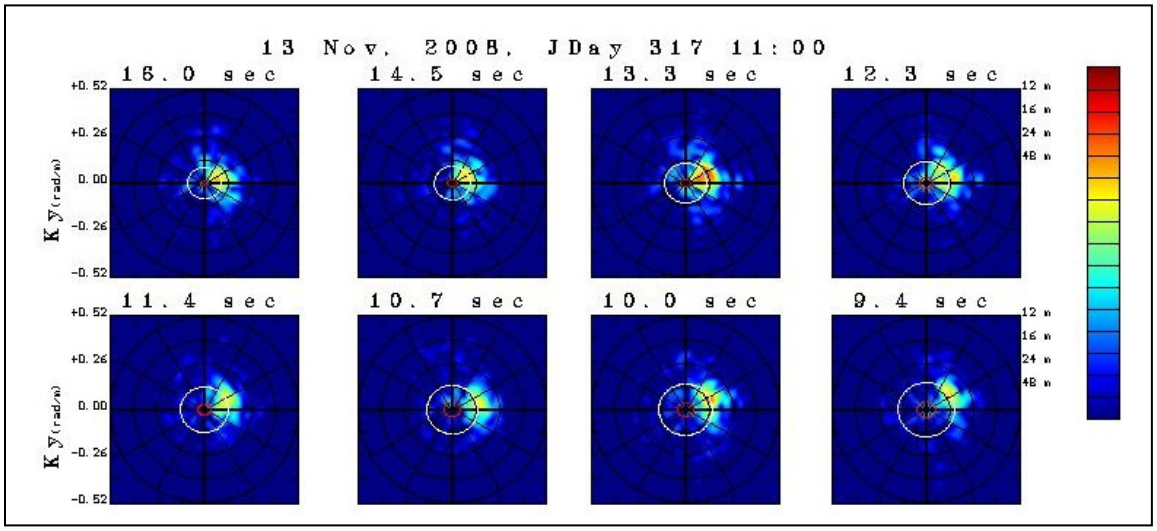

Fig. 3. Eight of 32 wave number spectra are plotted from 3D-FFT analysis of phase difference imagery of Fig.2, showing spectral energy peaking near 13.3-s period waves.

If the spectral peak energy is summed over a area of 3x3 pixels about each peak, then plotting these values results in a frequency spectrum for that area. Fig. 4 shows resulting frequency spectrum comparison with the pressure sensor array at the FRF for two time adjacent periods.

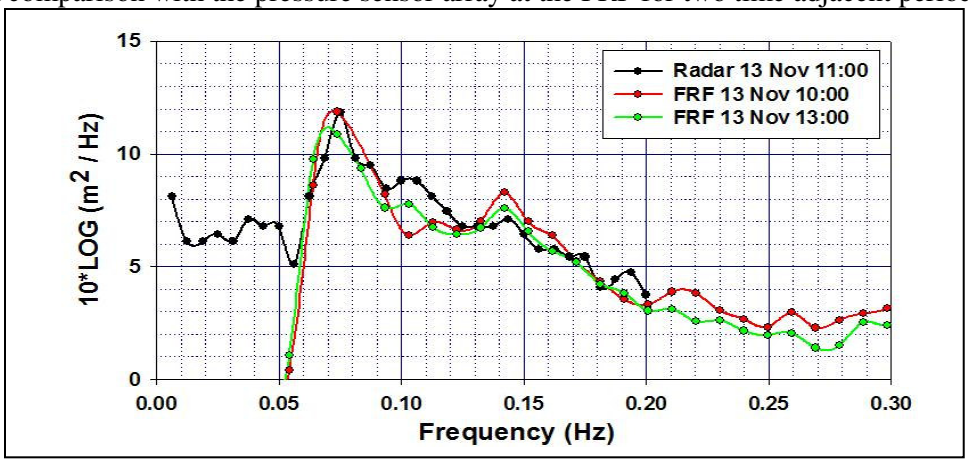

Fig. 4. Frequency spectrum derived from spectral peaks of 32 Kx,Ky spectra as in Fig. 3, with comparison results from FRF pressure-array spectrum for overlapping analysis periods.

5. ACKNOWLEDGEMENTS

The author wishes to acknowledge the support and hospitality provided by the U.S. Army Corps of Engineers, Field Research Facility personnel in this work, particularly Kent Hathaway, with whom we have a Co-operative Research and Development Agreement for this remote sensing application.

6. REFERENCES

[1] I.R.Young, W. Rosenthal, and F. Ziemer, "A three-dimensional analysis of marine radar images for the determination of ocean wave directionality and surface currents", *JGR*, vol. 90, pp. 1049-1059, 1985.

[2] D.B. Trizna, "Errors in Bathymetric Retrievals using Linear Dispersion In 3D FFT Analysis of Marine Radar Ocean Wave Imagery," IEEE Trans. Geosciences and Remote Sensing, **39**, pp. 2465-2469, 2001.

[3] H. Dankert and W. Rosenthal, "Ocean surface determination from X-band radar-image sequences," *JGR*, vol. 109, C04016, 2004.

[4] J. C. Nieto-Borge, G. R. Rodriguez, K. Hessner, and P. I. Gonzalez, "Inversion of marine radar images for surface wave analysis," *J. Atmos. Ocean. Tech.,* vol. 21, pp. 1291-1300, 2004.

[5] H. Dankert J. Horstmann, and W. Rosenthal, "Ocean Wind Fields Retrieved from Radar-Image Sequences", JGR Vol. 108, 2005.

[6] D. Lyzenga, O. Nwogu, D. Trizna, "Ocean wave field measurements using coherent and non-coherent radars at low grazing angles, *IGARSS 2010, Honolulu, HI,* 26-30 July, 2009.

[6] D.B. Trizna, "Monitoring coastal processes and ocean wave directional spectra using a marine radar" *Ocean Sciences 2006,Honolulu, HI,* 2-7 March, 2008.

[7] D.B. Trizna, "A coherent marine radar for decameter-scale current mapping and direct measurements of directional ocean wave spectra," *OCEANS 2008, Biloxi MI ,* pp.1-6, Sept. 2009.